Journal of the Iranian Chemical Society (2018) 15:1377–1389
https://doi.org/10.1007/s13738-018-1338-7

ORIGINAL PAPER

Novel Schiff base metal complexes: synthesis, characterization, DNA binding, DNA cleavage and molecular docking studies

Mayuri Bheemarasetti[1] · Kavitha Palakuri[1] · Shweta Raj[2] · Prakash Saudagar[2] · Durgaiah Gandamalla[3] · Narsimha Reddy Yellu[3] · Laxma Reddy Kotha[1]

Received: 1 September 2017 / Accepted: 23 February 2018 / Published online: 19 March 2018
© Iranian Chemical Society 2018

Abstract
A novel Schiff base, 3-(((1*H*-1,2,4-triazol-3-yl)imino)methyl)-4*H*-chromen-4-one (L) was synthesized and used as ligand for the synthesis of Co(II), Ni(II), Cu(II), Zn(II) and Pd(II) complexes. The structural characterization of the ligand and its metal complexes was determined by using various physicochemical and spectroscopic methods. The IR data show that the Schiff base ligand acts as a bidentate donor coordinating through the oxygen atom of the chromone and nitrogen atom of the imine group. Based on all spectral data, tetrahedral geometry has been proposed for all the metal complexes except Cu(II) and Pd(II) complexes. However, square-planar geometry has been proposed for Cu(II) and Pd(II) complexes. DNA binding interaction of the ligand and its metal complexes was investigated by using UV–visible absorption, fluorescence and molecular docking studies. The binding constants were in the order of 10^4 M^{-1} suggesting good binding affinity towards CT-DNA. The DNA cleavage activity of the synthesized compounds was investigated by using agarose gel electrophoresis. In vitro antimicrobial activity of the synthesized compounds were screened against two gram-positive bacteria (*Bacillus subtilis, Staphylococcus aureu*) and two gram-negative bacteria (*Escherichia coli, Proteus vulgaris*) and one fungi strain *Candida albicans* using disc diffusion method. Antioxidant activity was carried out by DPPH radical scavenging method. In vitro anti-proliferative activity of the ligand and its metal complexes was also carried on the HEK-293, HeLa, IMR-32 and MCF-7 cancer cell lines using MTT assay.

Keywords Schiff base metal complexes · DNA binding · DNA cleavage · Molecular docking · Anti-proliferative activity · Antioxidant

Introduction

In the recent decades, many natural and synthetic ligands containing nitrogen and oxygen as donor atoms have been presented in the literature. Most of the metal complexes reported in the literature are of ligands containing Schiff bases [1–5]. The Schiff base ligands are treated as the most significant ligands as they possess different coordinating atoms. Thus, the Schiff base ligands and their metal complexes have notable importance in the evaluation of the coordination chemistry [6]. However, synthesis of different Schiff base ligands with novel structure and properties are still an interesting research topic.

Chromone is the constitutional scaffold of different bioactive compounds of the synthetic as well as natural origin, and it has a great pharmaceutical importance [7, 8]. Synthetic point of view, 3-formylchromone has three electronic centres such as unsaturated keto function, a more active electrophilic centre at C_2 and a conjugated second carbonyl group at C_3. The synthesis of formylchromone Schiff base ligands and their coordination complexes shows higher biological activities such as antimicrobial, antiviral, anticancer, antioxidant, DNA binding and DNA cleavage [9–24]. For

Electronic supplementary material The online version of this article (https://doi.org/10.1007/s13738-018-1338-7) contains supplementary material, which is available to authorized users.

✉ Laxma Reddy Kotha
laxmareddychem12@gmail.com

[1] Department of Chemistry, National Institute of Technology, Warangal, Telangana 506 004, India

[2] Department of Biotechnology, National Institute of Technology, Warangal, Telangana 506 004, India

[3] Department of Pharmacology and Toxicology, Pharmaceutical Sciences, Kakatiya University, Warangal, Telangana 506009, India

example Bharath et al. and Ishar et al. reported formylchromone derivatives act as potent human colon cancer and topoisomerase inhibitor anticancer agents [25, 26]. They also have various kinds of applications in different areas like catalysts, analytical reagents, NLO materials, etc, [27–29]. Thus, it becomes an emerging area of interest for Inorganic Chemists in recent years. However, a limited work has been done on the metal complexes of 3-formylchromone Schiff bases [17, 30–40].

1,2,4-triazole and its derivatives belong to a class of exceptionally active compounds which possess a wide spectrum of biological properties, including antioxidant, antimicrobial, anti-inflammatory, anticonvulsant, antihypertensive and anti-HIV [41–44]. Moreover, some of the metal complexes of substituted 1,2,4-triazole ligands are widely used as molecular-based memory devices or optical sensors [45, 46]. Keeping this in view, we have selected a new Schiff base ligand, *i.e.,* 3-(((1*H*-1,2,4-triazol-3-yl)imino) methyl)-4*H*-chromen-4-one (L) for the synthesis of metal complexes. The synthesized metal complexes are characterized by using various spectral techniques and studied their biological activities.

Experimental

Materials

Dimethylformamide, phosphorousoxychloride, 2-hydroxyacetophenone, 3-amino-1,2,4-triazole and the metal acetates of cobalt(II), nickel(II), copper(II) and zinc(II) and palladium(II) chloride used were of AR grade, Sigma-Aldrich. The solvents such as methanol, acetone, dimethyl sulphoxide (DMSO) used were of spectroscopic grade, Merck. Calf thymus DNA (CT-DNA) was purchased from Himedia, Hyderabad, India.

Instruments

FTIR spectra of the synthesized compounds were recorded on PerkinElmer 100S spectrometer using KBr pellets. Elemental analysis was performed using a PerkinElmer CHN analyser. Melting points were recorded on Stuart SMP30. The electronic spectra were recorded on PerkinElmer UV–visible Spectrophotometer Lambda 25 in DMSO. Magnetic moments were determined on a Sherwood Scientific magnetic moment balance (Model No: MK1) at room temperature (25 °C) using $Hg[Co(SCN)_4]$ as a calibrant. Diamagnetic corrections were calculated using Pascal's constants. ^{1}H and ^{13}C NMR spectra of the ligand (L) were recorded in $CDCl_3$ solvent on Bruker Avance III New 500 MHz spectrometer. Mass data of the ligand were recorded on ESI-QToF (Waters Synapt G2S) high-resolution mass spectrometer. Thermogravimetric measurements of metal complexes were recorded on PerkinElmer diamond TGA instrument. The ESR spectrum of Cu(II) complex was recorded using JOEL X-Band Electron Spin Resonance spectrometer at room temperature. The fluorescence spectra of the compounds were recorded on Horiba yvon Fluorolog Spectrophotometer. The X-ray powder diffraction analysis was carried out by using PANlytical, X'Pert Powder X-ray diffractometer with Cu K_α radiation. The diffraction data are integrated by using Nakamuta program. Scanning electron microscopy (SEM) was obtained for all the compounds using Tescan Vega-3 LMU electron microscope.

Synthesis of 3-(((1*H*-1,2,4-triazol-3-yl)imino) methyl)-4*H*-chromen-4-one (L)

Synthesis of Schiff base ligand 3-(((1*H*-1,2,4-triazol-3-yl) imino)methyl)-4*H*-chromen-4-one **(3)** was performed by stirring the hot methanolic solutions of 3-formylchromone **(1)** (1.74 g, 1 mM) and 3-amino-1,2,4-triazole **(2)** (0.84 gm, 1 mM) for 1 h [47]. The yellow coloured compound thus obtained was isolated by filtration and was re-crystallized in methanol. The experimental details are listed in Scheme 1.

Yield: 75%; M.p.: 189 °C; $C_{12}H_8N_4O_2$: Anal. Found: C, 60.01; H, 3.36; N, 23.32% Calc.: C, 60.00; H, 3.33; N, 23.33%. IR (KBr, ν/cm^{-1}): ν(C=O) 1673, ν(C=N) 1610. UV–Vis (DMSO) λ_{max}/cm^{-1} (ε/M^{-1} cm^{-1}): 30,959 (19,300), 25,641 (6020). ^{1}H NMR (400 MHz, $CDCl_3$, TMS): δ 11.48 (s, 1H); 9.31 (d, 1H); 9.29 (d, 1H); 8.66 (s, 1H); 7.61 (m, 2H); 7.14 (t, 1H); 7.03 (t, 1H) (Fig. S1). ^{13}C NMR (100 MHz, $CDCl_3$, TMS): δ 158.3, 154.8, 137.8, 132.0, 119.7, 119.3. ESI–MS (m/z): Calc.: 240: Found: 241 (Fig. S2a).

Synthesis of metal complexes

A hot methanolic solution of Schiff base ligand (2 mM) was added to a hot methanolic solution of metal acetate salts of Co(II), Ni(II), Cu(II) and Zn(II) and Pd(II) chloride (1 mM) ($PdCl_2$ solution in 0.1 M HCl was taken and treated with an equal volume of water) and refluxed for 4 h. After refluxing the reaction mixture, the solid complexes thus separated were filtered and washed with methanol and dried in vacuo.

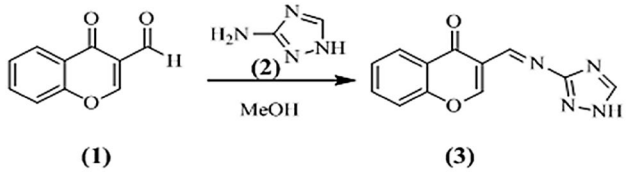

Scheme 1 Synthesis of Schiff base ligand (L)

$[CoL(OAc)_2]\cdot 2H_2O$: Brick red; Yield: 67%; M.p.: > 350 °C; $C_{16}H_{18}N_4O_8Co$: Anal. Found: C, 42.35; H, 3.97; N, 12.26; Co 13.09% Calc: C, 42.40; H, 4.00; N, 12.36; Co, 13.00%. Molar conductance (10^{-3} M DMF): 10 Ω^{-1} cm^{-1} mol^{-1}. IR (KBr, ν/cm^{-1}): ν(C=O) 1601, ν(C=N) 1574, ν(M–N) 475, ν(M–O) 533. UV–Vis (DMSO) λ_{max}/cm^{-1} (ε/M^{-1} cm^{-1}): 31,446 (13,150), 25,062 (13,170), 17,006 (170). μ_{eff} (BM): 4.73.

$[NiL(OAc)_2]\cdot 2H_2O$: Greenish yellow; Yield: 62%; M.p.: > 350 °C; $C_{16}H_{18}N_4O_8Ni$: Anal. Found: C, 42.38; H, 3.92; N, 12.39; Ni, 12.91% Calc: C, 42.42; H, 4.00; N, 12.37; Ni, 12.96%. Molar conductance (10^{-3} M DMF): 13 Ω^{-1} cm^{-1} mol^{-1}. IR (KBr, ν/cm^{-1}): ν(C=O) 1653, ν(C=N) 1578, ν(M–N) 482, ν(M–O) 557. UV–Vis (DMSO) λ_{max}/cm^{-1} (ε/M^{-1} cm^{-1}): 31,152 (17,700), 25,000 (19,900), 16,750 (211). μ_{eff} (BM): 2.91.

$[CuL(OAc)_2]\cdot 2H_2O$: Green; Yield: 77%; M.p.: > 350 °C; $C_{16}H_{18}N_4O_8Cu$: Anal. Found: C, 41.93; H, 3.91; N, 12.21; Cu; 13.82%. Calc.: C, 41.97; H, 3.96; N, 12.24; Cu, 13.88%. Molar conductance (10^{-3} M DMF): 9 Ω^{-1} cm^{-1} mol^{-1}. IR (KBr, ν/cm^{-1}): ν(C=O) 1600, ν(C=N) 1574, ν(M–N) 473, ν(M–O) 570. UV–Vis (DMSO) λ_{max}/cm^{-1} (ε/M^{-1} cm^{-1}): 25,125 (14,608), 14,641 (50). ESR: $g| = 2.33$, $g_{\perp} = 2.15$, G = 2.21. μ_{eff}(BM): 2.01. ESI MS (m/z): Calc.: 458. Found: 458 $[M^+]$.

$[ZnL(OAc)_2]\cdot H_2O$: Yellow; Yield: 60%; M.p.: > 350 °C; $C_{16}H_{16}N_4O_7Zn$: Anal. Found: C, 41.80; H, 3.72; N, 12.48; Zn, 14.23% Calc: C, 43.51; H, 3.65; N, 12.68; Zn, 14.80%. Molar conductance (10^{-3} M DMF): 18 Ω^{-1} cm^{-1} mol^{-1}. IR (KBr, ν/cm^{-1}): ν(C=O) 1611, ν(C=N) 1573, ν(M–N) 482, ν(M–O) 557. UV–Vis (DMSO) λ_{max}/cm^{-1} (ε/M^{-1} cm^{-1}): 31,152 (41,200), 26,809 (47,400). ESI MS (m/z): Calc.: 442. Found: 465 $[M+Na]^+$ (Fig.S2b).

$[PdL(Cl)_2]\cdot 4H_2O$: Brown; Yield: 68%; M.p.: > 350 °C; $C_{12}H_{16}C_{l2}N_4O_6Pd$: Anal. Found: C, 29.32; H, 3.21; N, 11.32; Pd, 21.59% Calc: C, 29.44; H, 3.29; N, 11.44; Pd, 21.74%. Molar conductance (10^{-3} M DMF): 14 Ω^{-1} cm^{-1} mol^{-1}. IR (KBr, ν/cm^{-1}): ν(C=O) 1650, ν(C=N) 1578, ν(M–N) 475, ν(M–O) 562, ν(M – Cl) 354. UV–Vis (DMSO) λ_{max}/cm^{-1} (ε/M^{-1} cm^{-1}): 31,153 (19,500), 23,529 (5850) (Fig. S3).

DNA binding activity

UV–visible spectroscopic studies

The UV–visible absorption studies show the interaction of ligand and its metal complexes with CT-DNA. Experiments were performed in 5 mM Tris–HCl/50 mM NaCl buffer solution (pH = 7.2) as per the procedure published in literature [48]. The concentration of CT-DNA was determined by using the electronic absorbance at 260 nm (molar absorption coefficient 6600 M^{-1} cm^{-1}). The absorbance ratio at 260 and 280 nm (A_{260}/A_{280}) is 1.81, suggesting that the CT-DNA solution was sufficiently free of protein. The stock solutions were stored at 4 °C and were used within 4 days. The titrations were carried out by keeping the constant concentration (50 μM) of the ligand and its metal complexes and by varying the concentration of CT-DNA (0.026×10^{-4}–0.261×10^{-4} M). From the electronic absorbance titration data, the binding constant (K_b) of the synthesized compounds has been determined by adopting the equation [48]:

$$[DNA]/(\varepsilon_a-\varepsilon_f) = [DNA]/(\varepsilon_b-\varepsilon_f) + 1/K_b(\varepsilon_b-\varepsilon_f) \quad (1)$$

where ε_a is the 'apparent' extinction coefficient, which was obtained by calculating A_{obsd}/[Compound]. The term ε_f corresponds to the extinction coefficient of free (unbound), and ε_b corresponds to the fully bound complexes. A plot of $[DNA]/(\varepsilon_a - \varepsilon_f)$ v/s [DNA] will give a slope $1/(\varepsilon_b - \varepsilon_f)$ and an intercept $1/K_b$ $(\varepsilon_b - \varepsilon_f)$. K_b is the ratio of the slope and the intercept.

Fluorescence spectroscopic studies

Compounds binding to DNA by intercalation mode were given through the emission quenching experiment. EB is a common fluorescent probe for DNA structure and has been selected for the examinations of the mode and process of compound binding to DNA. A 3 mL solution of 2.0 μM DNA and 1×10^{-5} M EB was titrated by 2.5–12.5×10^{-5} M compound ($\lambda_{ex} = 520$ nm, $\lambda_{em} = 535.0$–750.0 nm). The quenching constant (k_q) values were calculated by using classical Stern–Volmer equation [49]:

$$F_0/F = k_q[Q] + 1 \quad (2)$$

where F_0 is the emission intensity in the absence of quencher, F is the emission intensity in the presence of quencher, k_q is the quenching constant and $[Q]$ is the quencher concentration. Plots of F_0/F versus $[Q]$ appear to be linear and k_q depends on temperature.

Molecular docking studies

The 3D coordinates of the synthesized molecules (ligand, its Cu(II) and Zn(II) complexes) were rendered using CHEMDRAW 3D and the structures were visually confirmed using UCSF Chimera [50]. The B-DNA dodecamer structure with sequence 5′-D $(CGCGAATTCGCG)_2$ and sequence id: 1BNA was retrieved from RCSB (http://www.rcsb.org). The molecules were energy minimized for 100 steps of steepest gradient using UCSF Chimera [50]. The docking studies were performed using AUTODOCK 4.2 [51] where in Gasteiger charges and Kollman charges were distributed to the molecules and the B-DNA structures, respectively. The grid box was set to 0.375 Å. Genetic algorithm was chosen

for docking, and 50 GA runs were performed. The population size was set to 150, and the maximum number of generation was set to 27,000 in the GA parameters. The docked confirmations were then analysed for hydrogen bonding and binding energy.

Cleavage studies of pET28a plasmid DNA

Plasmid DNA cleavage experiments were performed according to the literature [52, 53]. Plasmid DNA cleavage ability of ligand and its metal complexes in the absence and presence of oxidant H_2O_2 was observed by agarose gel electrophoresis method. Stock samples of ligand and its complexes were prepared in DMSO (1 mg/mL). 100 µg/mL solutions were prepared by using Tris–HCl buffer from the stock solution. From that 15 µL was added to the isolated pET28a plasmid DNA of *E. coli*. The samples were incubated for 2 h at 37 °C, after that 1 µL of loading buffer (bromophenol blue in H_2O) was added to each sample and the mixed samples were loaded carefully into the 0.8% agarose gel electrophoresis chamber wells along with control (DNA alone). The electrophoresis was carried out at constant 70 V of electricity for 2 h. The gel was removed and stained with 10.0 mg/mL ethidium bromide for 10–15 min, and the bands were observed under Mediccare gel documentation system.

Antimicrobial activity

To study the antibacterial and antifungal activities of the ligand (L) and its metal complexes, they were tested against two gram-positive bacteria (*Bacillus subtilis, Staphylococcus aureu*) and two gram-negative bacteria (*Escherichia coli, Proteus vulgaris*) and one fungi strain *Candida albicans* using disc diffusion method. By using Whatman No. 1 paper, 6-mm-diameter sterile antibiotic discs were placed over the nutrient agar medium. By using micropipette, 100 µg/mL concentrated compounds were transferred to each disc (initially compounds are dissolved in 5% DMSO). Subsequently bacteria and fungi incubated overnight at 37 and 25 °C, respectively. The zone of inhibition was determined in mm and distinguished with standard antibiotics. DMSO was used as a negative control, whereas Kanamycin 30 µg/disc (standard antibiotic) and standard antifungal drug Clotrimazole (10 µg/disc) were used as the positive controls. All the tests were carried out in triplicates, and the average zones of inhibition were recorded and minimum inhibitory concentration values (MIC) calculated.

DPPH scavenging activity

The antioxidant activity of the synthesized compounds were determined by using 1,1-diphenyl-2-picrylhydrazyl (DPPH) free radical scavenging method as per the procedure given in the literature [54]. In the spectrophotometric assay, the capability to scavenge the stable free radical DPPH is determined by the absorbance at 517 nm. Synthesized compounds were initially dissolved in a minimum amount of DMSO and then in methanol (1 mg/mL) and these are used as stock solutions. From the stock solution, 1 mL of each test sample solution with different concentrations (25–100 µg) was added to the 3 mL of methanolic DPPH (0.004%) solution. After 30 min, the absorbance of the test compound was taken at 517 nm using UV–visible spectrophotometer. Methanol was used as blank, and BHT (butylated hydroxytoluene) was used as standard, and DPPH solution was used as control without the test compounds. The percentage of scavenging activity of DPPH free radical was measured by using the following formula:

$$\text{Scavengingactivity}(\%) = \left[\frac{(A_o - A_i)}{A_o}\right] \times 100 \quad (3)$$

where A_o corresponds to absorbance of the control and A_i corresponds to absorbance of the sample and accordingly IC_{50} values were calculated.

Anti-proliferative activity

In vitro anti-proliferative activity of the synthesized compounds was assayed against HEK-293, HeLa, IMR-32 and MCF-7 cell lines using MTT assay. The adherent cells were trypsinized as stated by the protocol, and after centrifugation they were resuspended in newly prepared medium. By pipetting, the cell suspension was carefully mixed to get a homogeneous single-cell suspension. Different concentrations of drug solutions were prepared in media with the final concentration of the DMSO in the well was to be < 1%. In each well of a 96-well plate, 100 µL of cell suspension was transferred aseptically and to it 100 µL of 1% drug solution (in quadruplicate) in media was added. At 37 °C, this plate was incubated for 72 h in CO_2 incubator. 20 µL of MTT was added to each well after 72 h of incubation period. Again the plate was incubated for 2 h. To the each well of the plate, 80 µL of lysis buffer was added and it was covered in aluminium foil to prevent the oxidation of the dye and it was placed on a shaker for overnight. On the ELISA reader at 562 nm wavelength absorbance was recorded. To find out the % inhibition of the test, absorbance was compared with that of DMSO control.

Results and discussion

All the complexes were soluble in DMF and DMSO. The molar conductance of the complexes (10^{-3} M DMF solution) is in the range 09–20 Ω^{-1} cm^2 mol^{-1} suggesting that these metal complexes are non-electrolytes [55].

Infrared spectra

The IR spectral information of ligand and its metal complexes was compared to find out the coordination sites that possibly participated in coordination with metal complexes. The important IR data of the ligand (L) and its metal complexes are listed in Table 1. In the Schiff base ligand (Fig. S4), the most predominant characteristic band of azomethine group (C=N) occurred at 1610 cm^{-1} and in its metal complexes this band was shifted to lower wave number by 32–37 cm^{-1}, which indicates the participation of nitrogen atom of azomethine group in coordination with metal ion [56]. The Schiff base ligand (L) shows a strong band at 1673 cm^{-1} due to the carbonyl group (C=O) of the chromone moiety. This band also shifted around 20–73 cm^{-1} to lower wave numbers in all the metal complexes. The shift in wave number indicates the involvement of oxygen atom of the carbonyl group in coordination with the metal ions [57]. NH group of the triazole ring was observed at 3072 cm^{-1} in ligand and its metal complexes, which indicates the non-involvement of NH group of the triazole ring [58]. All the metal complexes, except Pd(II), show bands at around 1510, 1450, 1340 and 710 cm^{-1} which can be assigned to ν_{as}(COO), ν_s(COO), δ(CH3) and δ(OCO) vibrations suggesting the presence of acetate ion in the coordination sphere [59]. However, a band at 354 cm^{-1} in Pd(II) complex indicates the presence of Pd–Cl bond. From the far infrared spectral bands in the range 600–400 cm^{-1} further confirms the participation of oxygen and nitrogen atoms in coordination with metal ions (i.e., ν(M–N) and ν(M–O)). The IR spectral data confirm all the metal ions coordinated by Schiff base ligand in a bidentate manner over oxygen and nitrogen atoms of the carbonyl and azomethine groups, respectively.

Electronic spectra and magnetic measurements

Generally the electronic absorption studies and magnetic measurements provide quick and reliable information about the geometry of metal complexes. These data can serve as effective tool to differentiate the tetrahedral,

Table 1 Important infrared frequencies (in cm^{-1}) of ligand (L) and its complexes

Compound	ν(C=O)	ν(C=N)	ν(M–N)	ν(M–O)	ν(M – Cl)
L	1673	1610			
$[CoL(OAc)_2]\cdot 2H_2O$	1601	1574	475	533	
$[NiL(OAc)_2]\cdot 2H_2O$	1653	1578	482	557	
$[CuL(OAc)_2]\cdot 2H_2O$	1600	1574	473	570	
$[ZnL(OAc)_2]\cdot H_2O$	1611	1573	482	557	
$[PdL(Cl)_2]\cdot 4H_2O$	1650	1578	475	562	354

Table 2 Electronic spectral data and magnetic moments of Schiff base ligand and its metal complexes

Compound	Band position (cm^{-1})	Transition	Geometry	μ_{eff} (BM)
L	25,641 30,959	LNCT LNCT		
$[CoL(OAc)_2]\cdot 2H_2O$	17,006 25,062 31,446	$^4A_2(F) \rightarrow {}^4T_1(P)$ LNCT LNCT	Tetrahedral	4.73
$[NiL(OAc)_2]\cdot 2H_2O$	16,750 25,000 31,152	$^3T_1(F) \rightarrow {}^3T_1(P)$ LNCT LNCT	Tetrahedral	2.91
$[CuL(OAc)_2]\cdot 2H_2O$	12,642 18,484 24,937	$^2B_{1g} \rightarrow {}^2E_g$ $^2B_{1g} \rightarrow {}^2B_{2g}$ LNCT	Square planar	2.01
$[ZnL(OAc)_2]\cdot H_2O$	26,809 31,152	LNCT LNCT	Tetrahedral	Diamagnetic
$[PdL(Cl)_2]\cdot 4H_2O$	23,529 30,769	$^1A_{1g} \rightarrow {}^1E_g$ LNCT	Square planar	Diamagnetic

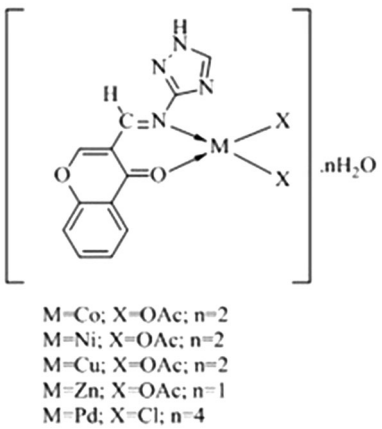

Fig. 1 Proposed structure of metal complexes

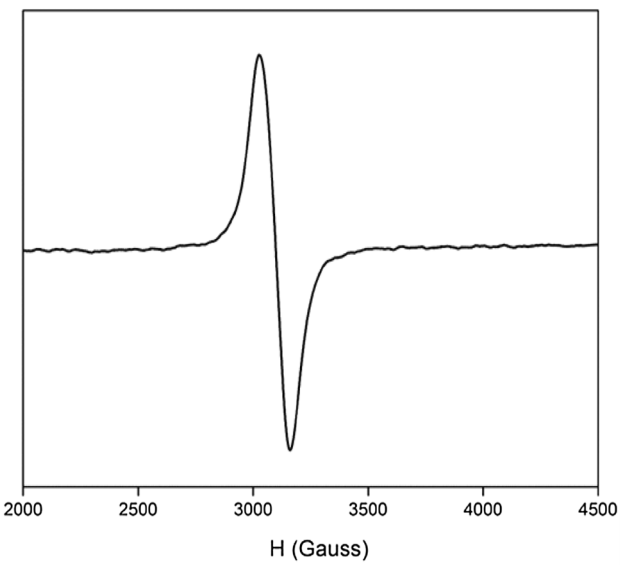

Fig. 2 ESR spectrum of Cu(II) complex

square-planar or octahedral geometries of the transition metal complexes. The absorption region, band assignment, magnetic moment and the proposed geometry of the complexes are given in Table 2. Based on these data, a tetrahedral geometry has been assigned to all complexes except Cu(II) and Pd(II) complexes which have square-planar geometry (Fig. 1). These values are comparable with other reported complexes in the literature [60–68].

ESR spectra

ESR spectrum of Cu(II) complex was recorded in benzene solution at room temperature (Fig. 2). The Cu(II) complex showed a band centred at g = 2.21 with unresolved hyperfine structure. The values of $g\|$ and $g_{\perp}$ are 2.33 and 2.15 ($g\| > g_{\perp} > 2.0023$), showing that the unpaired electron in the ground state of Cu(II) predominately lies in $d_{x^2-y^2}$ orbital, this was referring to a square-planar geometry around Cu(II) ions [69]. The most significant factor is that the $g\|$ value (2.33) is considerably greater than most of the common Cu(II) complexes. A factor potentially contributing to increase of $g\|$ is distortion from square-planar geometry [70]. From the obtained values, it is shown that $A\|$ (133) > $A_{\perp}$ (21); $g\|$ (2.33) > $g_{\perp}$ (2.21) > 2.0023. The g-values in the axial spectra are connected with exchange interaction coupling constant (G). From the G value, ligand nature is also evaluated by the expression

$$G = \frac{g\,\| - 2.0023}{g\perp - 2.0023} \tag{4}$$

As reported by Karlin and Zubieta [70], if the G value is more than four, the exchange interaction is insignificant because the local tetragonal axes are aligned parallel or are slightly misaligned. If the G value is smaller than four, the exchange interaction is reasonable and the local tetragonal axes are misaligned. The noticed value for the exchange interaction parameter for the copper complex ($G = 2.216$) recommends that the ligand forming complex is observed as a strong field, and the local tetragonal axes are misaligned, and the exchange coupling effects are not operative in the present copper(II) complex. The metal–ligand bonding in this complex is covalent. It also further suggests that the stereochemistry of Cu(II) complex is square planar [69]. The degree of geometrical distortion was ascertained by a parameter $g\|/A\|$ ($A\|$ in cm^{-1}) with the values < 140 cm^{-1} associated with the square-planar structure, whereas higher values indicate distortion towards tetrahedron. In the current Cu(II) complex $g\|/A\|$ value is 175 cm^{-1} which indicates the distortion in the complex [71].

Thermogravimetric studies

TG graphs of Co(II) and Ni(II) complexes of the ligand (L) are shown in Fig. 3. All the metal complexes were decomposed in two steps. The first step occurs in the temperature range between 60 and 120 °C with a weight loss of 3–15% which corresponds to the loss of lattice water molecules. In the second step, the total loss of ligand molecules was observed in the temperature range between 120 and 600 °C. Finally, metal oxide as a residue was observed.

Fluorescence spectra

The solid-state emission spectra of the ligand (L) and its Zn(II) complex are given in Fig. 4. Schiff base ligand and its

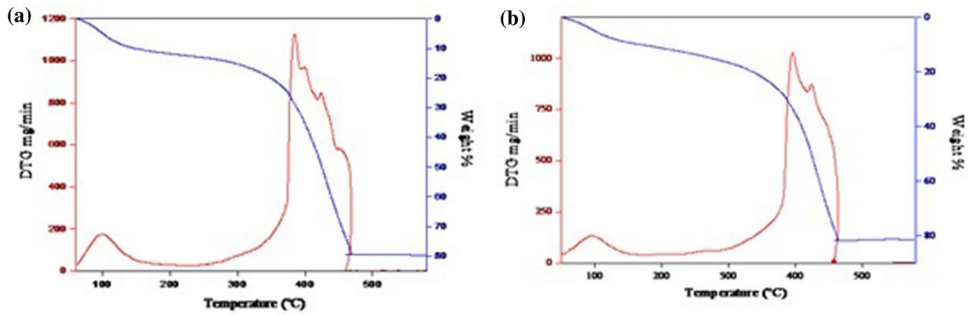

Fig. 3 TG-DTG graphs of **a** Co(II) complex and **b** Ni(II) complex

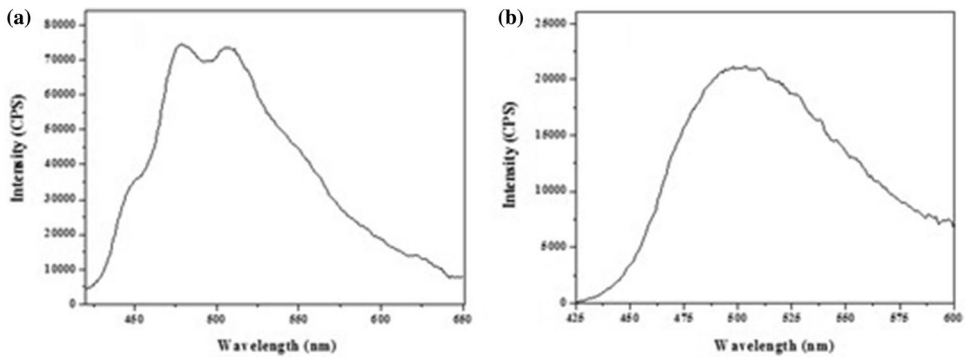

Fig. 4 Emission spectra of **a** Schiff base ligand (L) **b** its Zn(II) complex

Zn(II) complex exhibited fluorescence property but remaining metal complexes (Co(II), Ni(II), Cu(II) and Pd(II)) do not exhibit any emission bands. The ligand was characterized by two emission bands at around 478 and 508 nm, and its Zn(II) complex shows emission band at 496 nm upon photo-excitation at 400 nm. There was a decrease in the intensity of the emission band of Zn(II) complex when compared to the ligand. Literature reports revealed that there was a decrease/increase in fluorescence intensity or quenching or new emission bands are observed especially when the ligand is bonded with transition metals [29, 72, 73].

Powder XRD and SEM

The powder X-ray diffraction data for the synthesized compounds were obtained for structural characterization purpose. Powder XRD pattern of the compounds was recorded over the $2\theta = 10°–80°$. The powder XRD patterns of the Schiff base ligand and its Pd(II) complex are shown in Fig. 5. Observed and calculated powder XRD data of the Schiff base ligand and its Pd(II) complex are given in Table S1 (a&b) in Supplementary Information.

Except Co(II), Ni(II) and Cu(II) complexes, the Schiff base ligand and its Zn(II) and Pd(II) complexes displayed sharp crystalline peaks indicating their crystalline nature. However, Co(II), Ni(II) and Cu(II) complexes are in amorphous nature. The Schiff base ligand and its Zn(II) and Pd(II) complexes were monoclinic with distinct unit cell parameters. Unit cell parameters of ligand and its Zn(II) and Pd(II) complexes were as follows: *L*: $a = 6.8684$ Å, $b = 12.9430$ Å, $c = 7.6223$ Å, $\beta = 95.128°$. $V = 674.89$ Å^3; $[ZnL(OAc)_2]\cdot H_2O$: $a = 8.5103$ Å, $b = 10.1787$ Å, $c = 11.7909$ Å, $\beta = 94.898°$. $V = 1017.63$ Å^3; $[PdL(Cl)_2]\cdot 4H_2O$: $a = 7.2840$ Å, $b = 15.3626$ Å, $c = 12.9642$ Å, $\beta = 96.933°$, $V = 1440.11$ Å^3. By using Debye–Scherrer's formula, the average crystallite sizes for all compounds are determined [74]. The ligand and its Zn(II) and Pd(II) complexes have an average crystallite size of 36, 24 and 10 nm, respectively, indicating that the compounds were in nanocrystalline phase.

The SEM micrographs of the synthesized ligand and its complexes were taken to analyse their morphology and grain size. The SEM–EDS micrographs of the Ni(II) complex are shown in Fig. 6. From the SEM micrographs, it is observed that there was a uniform matrix in the ligand and its complexes, which implies their homogeneous nature. The SEM images of ligand and its Cu(II) and Pd(II) complexes show agglomerated thin plates, ice granular and ice plates like morphologies. However, Co(II), Ni(II) and Zn(II) complexes showed spherical-shaped particles, with an average grain size of 0.52, 0.59 and 0.95 µm, respectively. (SEM images of (1) Ligand, (2) Co(II) complex, (3) Zn(II) complex, (4) Pd(II) complex are presented in Fig. S5 Supplementary Information).

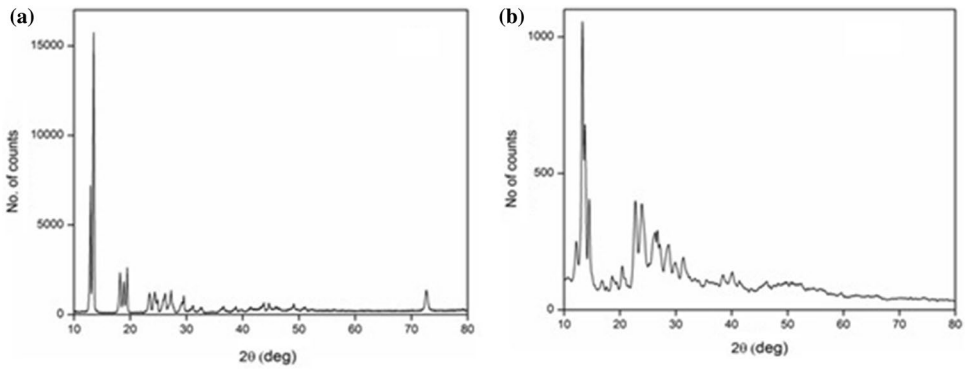

Fig. 5 Powder XRD spectra of **a** Schiff base ligand (L) **b** Pd(II) complex

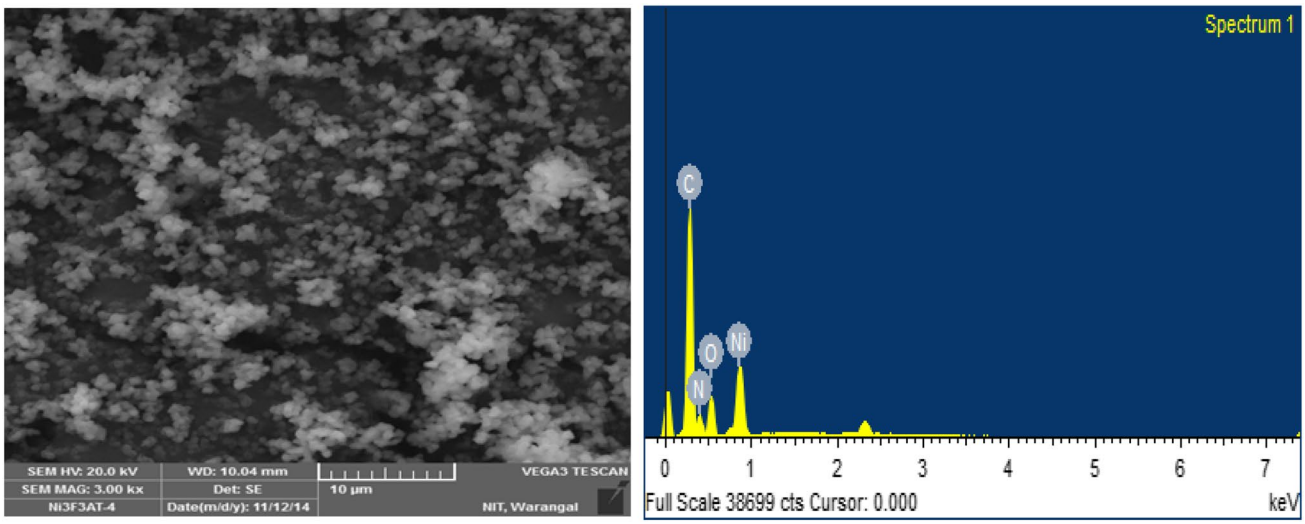

Fig. 6 SEM micrograph and EDX of Ni(II) complex

DNA binding activity

UV–visible spectroscopic studies

The potential DNA binding ability of the synthesized compounds was characterized by UV–visible absorption spectroscopy. This is one of the most useful methods in DNA binding studies [75]. Absorption studies shows that the compounds can bind to DNA either through covalent bonding, such as in complexes that contain ligands that can be substituted with the nitrogen base of DNA [76], or by non-covalent interactions such as electrostatic and intercalation or groove binding [77]. When the concentration ($0–0.261 \times 10^{-4}$ M) of the compounds was increased, hypochromism of the absorption bands was observed. The results suggest that the compounds bind to DNA by intercalative, since intercalation leads to hypochromism in the spectral bands [78]. There was a red shift observed for Co(II), Zn(II) and Pd(II) complexes, which indicates the stabilization of the DNA duplex due to an intimate association between complexes and DNA. The electronic spectra of ligand and its Zn(II) complex in the absence and presence of increasing amount of DNA (at a constant concentration of complexes) are given in Fig. 7.

The binding constant K_b values obtained for ligand, Co(II), Ni(II), Cu(II), Zn(II) and Pd(II) complexes were 2.8×10^4 M^{-1}, 3.6×10^4 M^{-1}, 3.5×10^4 M^{-1}, 4.8×10^4 M^{-1}, 3.7×10^4 M^{-1} and 2.0×10^4 M^{-1}, respectively. Hypochromism and redshift clearly indicate that there was an interaction between metal complexes and DNA. The results also show that the binding magnitudes of the metal complexes with DNA lie in the following order Pd(II) < Ni(II) < Co(II) < Zn(II) < Cu(II). The greater K_b value of Cu(II) complex indicates its strong binding with DNA.

Fluorescence quenching studies

The fluorescence quenching spectrum of DNA–EB system by the ligand and its Zn(II) complex is shown in Fig. 8. The fluorescence emission intensity of the DNA–EB system decreased with the increase in the compound concentration. The resulting decrease in fluorescence is caused by EB changing from a hydrophobic environment to an aqueous environment. Such a characteristic change is often observed in intercalative DNA interactions. The quenching plots illustrate that the quenching of EB bound to DNA by the ligand and its complexes were in good agreement with the linear Stern–Volmer equation. In the plots of F_0/F versus [Q], k_q is given by the ratio of the slope to the intercept. The k_q values for the ligand, Co(II), Ni(II), Cu(II), Zn(II) and Pd(II) complexes were $1.22 \times 104\ M^{-1}$, $5.25 \times 104\ M^{-1}$, $4.95 \times 104\ M^{-1}$, $2.32 \times 105\ M^{-1}$, $8.32 \times 104\ M^{-1}$ and $3.20 \times 104\ M^{-1}$, respectively. This data suggest that the interaction of the Cu(II) complex with CT-DNA is stronger than that of the remaining complexes, which is consistent with the above absorption spectral results.

The Pearson correlation between the binding constants K_b and k_q is calculated and shown in Fig. 9. The correlation coefficient value (r) is 0.84, indicating that there is a strong linear relationship between the variables.

Molecular docking studies

The docking results of the compounds (ligand, Cu(II) and Zn(II) complexes) were analysed for binding with major and minor groove of B-DNA (Fig. 10), and furthermore the hydrogen bonding to the nucleotides was also checked. Table S2 shows the distribution of each of the compounds in 50 runs to the major groove, minor groove, H-bonds to ATGC, and maximum binding energies were recorded.

The H-bonds showed that the compounds were distributed along the major and minor groves almost equally. All the compounds revealed higher affinity towards purines especially guanine. The presence of carboxyl oxygen which has higher electronegativity in the compounds causes disruption of hydrogen bonds between nucleotide base pairs. The results of molecular docking study show that the compounds bind efficiently with the DNA receptor (in minor groove) and their binding energy values − 7.66, − 9.39 and − 12.26 kcal mol^{-1} for ligand, Cu(II) and Zn(II) complexes, respectively. The more negative of binding energy indicated its strong binding ability to the DNA. Among the compounds, Zn(II) complex displayed higher binding affinity towards the DNA molecule and also contributed to most of the hydrogen bonds to guanine. Therefore, Zn(II) complex has a better chance of disrupting DNA molecules and causing mutation. These molecules stand a chance as a drug

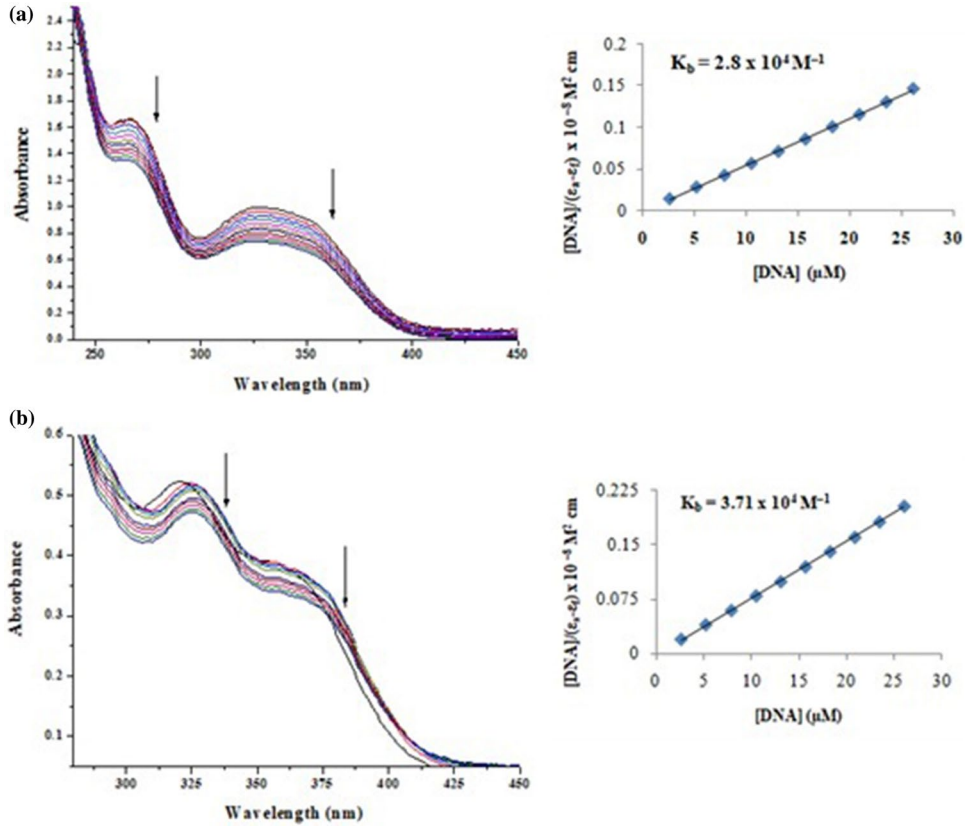

Fig. 7 Absorption spectra of the **a** ligand (L) and **b** Zn(II) complex upon addition of CT-DNA. [Compound] = 50 μM, [DNA] = 0.026×10^{-4} M to 0.261×10^{-4} M. Arrow shows the absorbance changes upon increasing DNA concentration

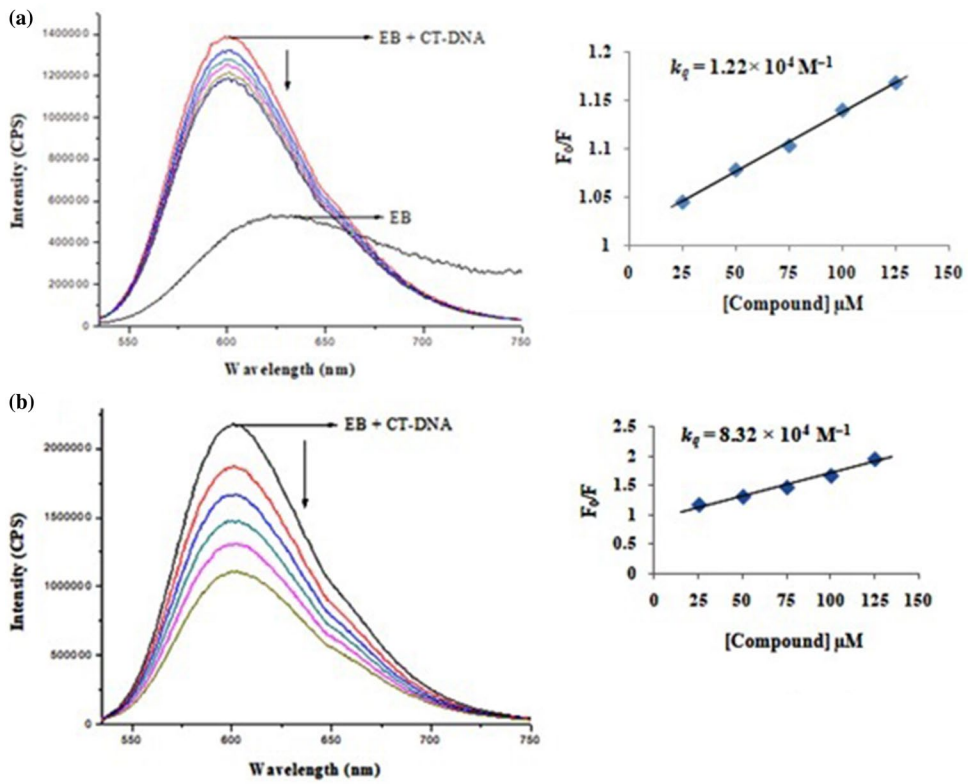

Fig. 8 Emission spectra of EB bound to DNA in the absence and presence of **a** ligand **b** Zn(II) complex (25–125 µM) and plot of F_0/F versus [Q]

molecule towards treating cancer and also as DNA-targeted drug delivery systems.

Cleavage of plasmid pET28a DNA

The cleavage of pET28a plasmid DNA with the synthesized compounds in absence and presence of H_2O_2 has been monitored by agarose gel electrophoresis as shown in Fig. 11a, b. The mechanism of nucleolytic activity of synthesised compounds has been investigated. DNA alone (Control) does not show activity. In the absence of H_2O_2 (Fig. 11a), observed molecular weight difference in all lanes compared to control indicates their partial nucleolytic activity. Probably this may be due to the redox behaviour of the metal ions. These results indicated the important role of the metal ions in cleavage studies. In the presence of H_2O_2 (Fig. 11b), absence of marker bands was clearly observed in Cu(II) and Zn(II) complexes indicate the complete DNA cleavage activity. In the case of Co(II), Ni(II) and Pd(II) complexes, a decrease in the intensity of bands was observed compared to the control. This is probably due to the partial cleavage of the DNA. As a result, in the presence of oxidant DNA cleavage activity was more when compared with the absence of oxidant. It may be due to the formation of hydroxyl radicals. The general oxidative DNA cleavage mechanism was proposed in the literature by several research groups [73]. Compounds were observed to cleave the DNA, concluding that the compounds inhibit the growth of the pathogenic organism by cleaving the genome.

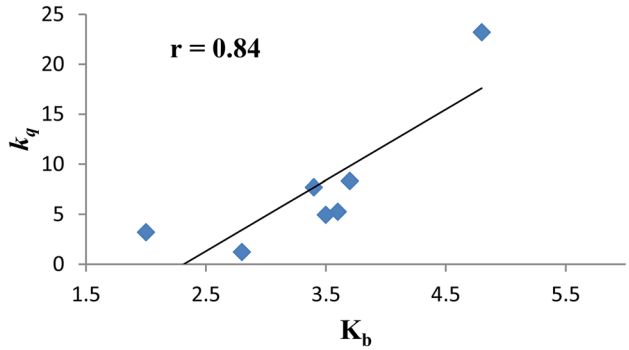

Fig. 9 Pearson correlation between the binding constants K_b and k_q

Antimicrobial activity

The microbial results of the synthesized compounds in minimum inhibitory concentration (MIC) are given in Table 3. Ligand and its Cu(II) and Zn(II) complexes showed moderate activity against tested microorganisms, and they were compared with the standard drugs (kanamycin and clotrimazole). However, remaining metal complexes (Co(II), Ni(II) and Pd(II)) did not show any activity against tested microorganisms. The higher activity of the metal complexes

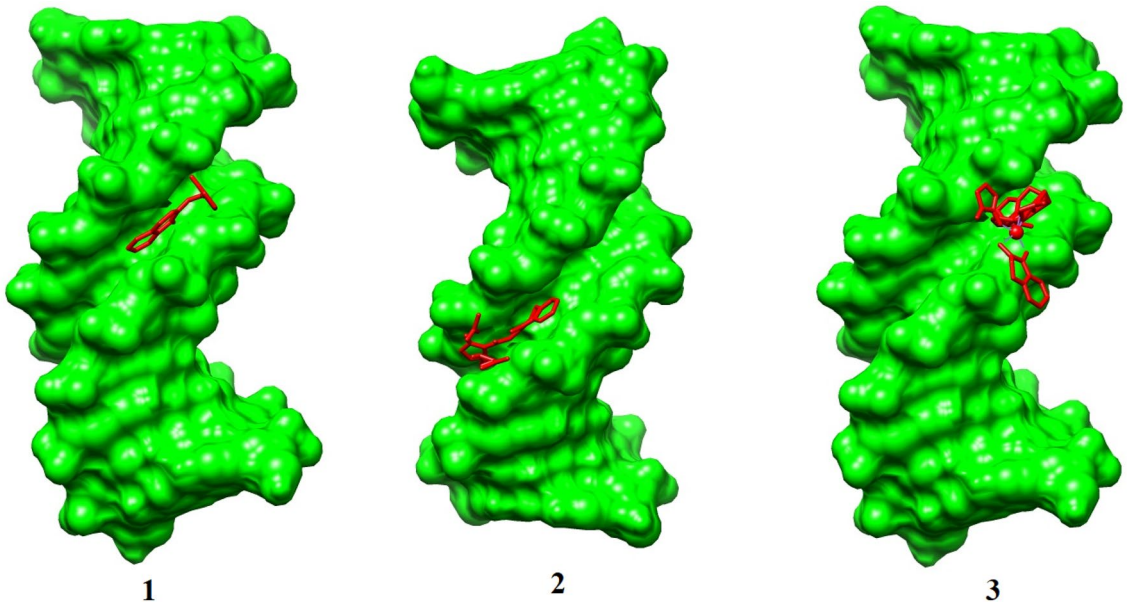

Fig. 10 Molecular docked model of Schiff base ligand (1), Cu(II) complex (2) and Zn(II) complex (3) with BDNA dodecamer structure with sequence 5′-D $(CGCGAATTCGCG)_2$ and sequence id: 1BNA

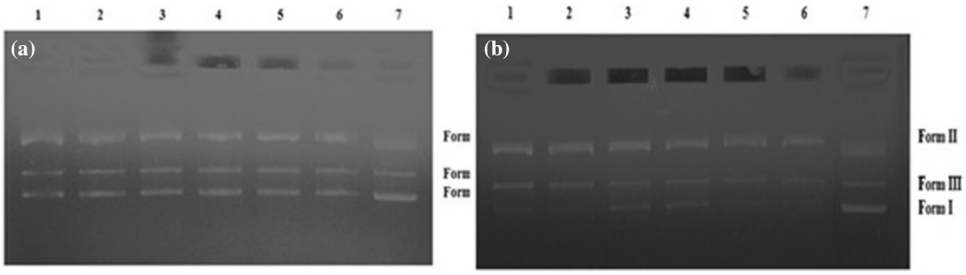

Fig. 11 Gel electrophoresis photograph of ligand (L) and its metal complexes in the absence of H_2O_2 (**a**) and presence of H_2O_2 (**b**). **a** Lane 1: DNA + Ligand, Lane 2: DNA + Cu(II) complex, Lane 3: DNA + Co(II) complex, Lane 4: DNA + Ni(II) complex, Lane 5: DNA + Zn(II) complex, Lane 6: DNA + Pd(II) complex and Lane 7: Control (DNA alone). **b** Lane 1: DNA + Ligand + H_2O_2, Lane 2: DNA + Cu(II) complex + H_2O_2, Lane 3: DNA + Co(II) complex + H_2O_2, Lane 4: DNA + Ni(II) complex + H_2O_2, Lane 5: DNA + Zn(II) complex + H_2O_2, Lane 6: DNA + Pd(II) complex + H_2O_2 and Lane 7: Control (DNA alone)

can be explained based on the Overtones concept and chelation theory [29]. According to these, chelation could allow for the delocalization of π-electrons over the entire chelate ring and enhances the lipophilicity of the complexes. This increased lipophilicity facilitates the penetration of the complexes into lipid membranes, further restricting proliferation of the microorganisms. The negative results can be attributed either to the inability of the complexes to diffuse into the bacteria cell membrane, and hence they become unable to interfere with its biological activity [74].

DPPH scavenging activity

2,2-Diphenyl-2-picrylhydrazyl (DPPH) assay is widely used for assessing the ability of radical scavenging activity, and it is measured in terms of IC_{50} values. DPPH is a well-known radical and a scavenger for other radicals. Therefore, DPPH radical was reduced in the presence of an antioxidant. The results revealed that the ligand ($IC_{50} = 1.35$ μg/mL (5.62 μM)) and its Ni(II) complex ($IC_{50} = 0.79$ μg/mL (1.74 μM)) exhibited significant activity. By increasing the concentration of the compounds, the scavenging activity was also increasing. However, remaining metal complexes (Co(II), Cu(II), Zn(II) and Pd(II)) have not shown any activity. From the data, it is also confirmed that the Ni(II)

Table 3 MIC values of antimicrobial activity of compounds (μg/mL)

Compound	*Bacillus subtilis*	*Staphylococcus aureus*	*Proteus vulgaris*	*Escherichia coli*	*Candida albicans*
L	50	60	40	60	70
$[CuL(OAc)_2]\cdot 2H_2O$	50	60	60	70	70
$[ZnL(OAc)_2]\cdot H_2O$	40	30	30	30	40
Kanamycin	10	7	8	9	–
Clotrimazole	–	–	–	–	10

Table 4 IC_{50} values of anti-proliferative activity of compounds (μg/mL)

Compound	MCF-7	HeLa	HEK-293	IMR-32
L	54.38118	59.24883	53.48518	56.6363
$[CoL(OAc)_2]\cdot 2H_2O$	54.95246	63.63953	51.40602	71.12986
$[NiL(OAc)_2]\cdot 2H_2O$	29.42310	82.48103	31.21530	34.61490
$[CuL(OAc)_2]\cdot 2H_2O$	20.21214	23.81992	25.39196	19.82635
$[ZnL(OAc)_2]\cdot H_2O$	30.29015	36.46410	29.22829	27.54759
$[PdL(Cl)_2]\cdot 4H_2O$	51.88243	58.63759	56.05024	58.94592
Cis-platin	11.44337	7.281537	11.90309	11.44337

complex was shown comparable activity to the standard drug BHT (IC_{50} = 0.67 μg/mL (3.04 μM)).

Anti-proliferative activity by MTT Assay

The cytotoxic effect of the new synthesized compounds on the proliferation of human cervical cancer cells (HeLa), neuroblastoma cells (HEK-293), normal kidney cells (IMR-32) and human breast cancer cells (MCF-7) was done by MTT assay. The IC_{50} values obtained for the synthesized compounds against the tested cell lines are listed in Table 4. The results show that the metal complexes exhibited good activity when compared to the ligand and lesser activity when compared to the standard drug. The greater activity of the complexes may be due to the chelation. However, Cu(II) complex exhibited higher activity when compared with the remaining metal complexes against all tested cell lines.

Conclusion

In this paper, Co(II), Ni(II), Cu(II), Zn(II) and Pd(II) complexes with Schiff base ligand (L) derived from 3-formylchromone and 3-amino-1,2,4-triazole have been synthesized and characterized. The ligand (L) acts as bidentate coordinating through oxygen and nitrogen atoms of azomethine and carbonyl group of pyrone ring, respectively, confirmed by spectral, analytical, thermal and magnetic studies. Acetate/chloride molecules are also coordinated to the metal ions. The Co(II), Ni(II) and Zn(II) complexes have shown tetrahedral geometry, whereas Cu(II) and Pd(II) complexes have shown square-planar geometry. Antimicrobial activity of the compounds showed moderate activity. The Ni(II) complex of the ligand showed comparable antioxidant activity to the standard BHT. The DNA binding results show that the compounds bind to CT-DNA via intercalative mode. The synthesized compounds have potent cleavage activity without any external reagents, but the cleavage activity is more when H_2O_2 is added as external oxidising agent. Cu(II) complex displayed good anti-proliferative activity compared to the remaining compounds. From all the results, Cu(II) and Zn(II) complexes can be used as a promising antitumor agents in vivo to inhibit the DNA replication in the cancer cells and not allow the tumour for further growth.

Acknowledgements The authors wish to thank the Director, CMET, Hyderabad, for providing TG facility. The authors are thankful to the Department of Biochemistry, SV University, Tirupati, for providing antioxidant activity, Department of Biotechnology and University College of Pharmaceutical Sciences, Kakatiya University, Warangal, for antimicrobial and anti-proliferative activity studies. We also wish to thank the Ministry of Human Resource Development for granting the research fellowship to B. Mayuri.

References

1. A.A.M. Belal, I.M. El-Deen, N.Y. Farid, R. Zakaria, M.S. Refat, Spectrochim. Acta A **149**, 771 (2015)
2. M. Salehi, M. Amirnasr, S. Meghdadi, K. Mereiter, H.R. Bijanzadeh, A. Khaleghian, Polyhedron **81**, 90 (2014)
3. S. Esmaielzadeh, L. Azimian, K. Shekoohi, H. Esfandiari, M. Asadi, Z. Zare, A. Rahmani Nejad, K. Mohammadi, Inorg. Chim. Acta **405**, 155 (2013)
4. M. Muthu Tamizh, R. Karvembu, Inorg. Chem. Commun. **25**, 30 (2012)
5. P. Mendu, C.G. Kumari, R. Ragi, J. Fluoresc. **25**, 369 (2015)
6. M. Montazerozohori, S.A. Musavi, A. Masoudiasl, A. Naghiha, M. Dusek, M. Kucerakova, Spectrochim. Acta A **137**, 389 (2015)
7. V.Y. Sasnovskikh, R.A. Irgashev, Tetrahedron Lett. **48**, 7436 (2007)
8. Z. Siddiqui, F. Farooq, J. Chem. Sci. **124**, 1097 (2012)
9. O.A. El-Gammal, G.A. El-Reash, S.F. Ahmed, J. Mol. Struct. **1007**, 1 (2012)

10. L. Puccetti, G. Fasolis, D. Vullo, Z.H. Chohan, A. Scozzafava, C.T. Supuran, Bioorg. Med. Chem. Lett. **15**, 3096 (2005)
11. J. Nawrot-Modranka, E. Nawrot, Acta Pol. Pharm. **63**, 429 (2007)
12. C. Anitha, C.D. Sheela, P. Tharmaraj, S. Johnson Raja, Spectrochim. Acta A **98**, 35 (2012)
13. J. Wang, Z.Y. Yang, X.Y. Yi, B.D. Wang, J. Photochem. Photobiol., A **201**, 183 (2009)
14. S.A. Elsayed, I.S. Butler, B.J. Claude, S.I. Mostafa, Transit. Metal Chem. **40**, 179 (2015)
15. Y. Li, Z. Yang, J. Coord. Chem. **63**, 1960 (2010)
16. M. Grazul, E. Budzisz, Coordin. Chem. Rev. **253**, 2588 (2009)
17. Y. Li, Z.Y. Yang, J. Fluoresc. **20**, 329 (2010)
18. J. Wang, Z.Y. Yang, B.D. Wang, X.Y. Yi, Y.C. Liu, J. Fluoresc. **19**, 847 (2009)
19. B.D. Wang, Z.Y. Yang, D.W. Zhang, Y. Wang, Spectrochim. Acta A **63**, 213 (2006)
20. D.D. Qin, G.F. Qi, Z.Y. Yang, J.C. Wu, Y.C. Liu, J. Fluoresc. **19**, 409 (2009)
21. B.D. Wang, Z.Y. Yang, P. Crewdson, D.Q. Wang, J. Inorg. Biochem. **101**, 1492 (2007)
22. K. Mansouri, R. Khodarahmi, A. Foroumadi, A. Mostafaie, H.M. Motlagh, Med. Chem. Res. **20**, 920 (2011)
23. S.X. Cai, J. Drewe, W. Kemnitzer, Anticancer Agents Med. Chem. **9**, 437 (2009)
24. H. Adibi, R. Khodarahmi, K. Mansouri, M. Khaleghi, S. Maghsoudi, Pharm. Sci. **19**, 23 (2013)
25. Z. Baráth, R. Radics, G. Spengler, I. Ocsovszki, M. Kawase, N. Motohashi, Y. Shirataki, A. Shah, J. Molnár, In Vivo **20**, 645 (2006)
26. P.S. Ishar, G. Singh, S. Singh, K.K. Sreenivasan, G. Singh, Bioorganic Med. Chem. Lett. **16**, 1366 (2006)
27. A.M.A. Hassan, A.I. Hanafy, M.M. Ali, A.A. Salman, Z.A. El-Shafay, Z.H. Abd El-Wahab, I.A. Salama, J. Basic Appl. Chem. **2**, 1 (2012)
28. A.K. Bishnoi, R. Dass, R.G. Sharma, Anal. Sci. **20**, 921 (2004)
29. M. Kalanithi, D. Kodimunthiri, M. Rajarajan, P. Tharmaraj, Spectrochim. Acta A **82**, 290 (2011)
30. P. Kavitha, M. Saritha, K. Laxma Reddy, Spectrochim. Acta A **102**, 159 (2013)
31. P. Kavitha, K. Laxma Reddy, Bioinorg. Chem. Appl. **2014** (2014)
32. P. Kavitha, K. Laxma Reddy, Arab. J. Chem. **9**, 596 (2016)
33. P. Kavitha, K. Laxma Reddy, Arab. J. Chem. **9**, 640 (2016)
34. P. Kavitha, M.R. Chary, B.V.A.A. Singavarapu, K. Laxma Reddy, J. Saudi Chem. Soc. **20**, 69 (2016)
35. V. Barve, F. Ahmed, S. Adsule, S. Banerjee, S. Kulkarni, P. Katiyar, C.E. Anson, A.K. Powell, S. Padhye, F.H. Sarkar, J. Med. Chem. **49**, 3800 (2006)
36. F. Arjmand, F. Sayeed, M. Muddassir, J. Photochem. Photobiol., B **103**, 166 (2011)
37. A.D. Kulaczkowska, J. Therm. Anal. Calorim. **109**, 7 (2012)
38. Y. Li, Z.Y. Yang, ZCh. Liao, Z.C. Han, Z.C. Liu, Inorg. Chem. Commun. **13**, 1213 (2010)
39. Y. Li, Z.Y. Yang, J.C. Wu, Eur. J. Med. Chem. **45**, 5692 (2010)
40. Y. Li, Z.Y. Yang, T.R. Li, Z.C. Liu, B.D. Wang, J. Fluoresc. **21**, 1091 (2011)
41. O. Bekircan, Z. Bıyıklıoglu, I. Acar, H. Bektas, H. Kantekin, J. Organomet. Chem. **693**, 3425 (2008)
42. J. Chen, X.Y. Sun, K.Y. Chai, J.S. Lee, M.S. Song, Z.S. Quan, Med. Chem. **15**, 6775 (2007)
43. O. Bekircan, B. Kahveci, O.B. Özgümüs, Chin. J. Chem. **25**, 1871 (2007)
44. R. Lesyka, O. Vladzimirska, S. Holota, L. Zaprutko, A. Gzella, Eur. J. Med. Chem. **42**, 641 (2007)
45. O. Kahn, C.J. Martinez, Devices Sci. **279**, 44 (1998)
46. Y. Garcia, P.J. Koningsbruggen, E. Codjovi, R. Lapouyeda, O. Kahn, L. Rabardel, J. Mater. Chem. **7**, 857 (1997)
47. A. Nohara, T. Umetani, Y. Sanno, Tetrahedron Lett. **14**, 1995 (1973)
48. N. Vamsikrishna, M. Pradeep Kumar, R. Kumar, G. Ramesh, N. Ganji, S. Daravath, J. Chem. Sci. **129**, 609 (2017)
49. M.R. Efink, C.A. Ghiron, Anal. Biochem. **114**, 199 (1981)
50. E.F. Pettersen, T.D. Goddard, C.C. Huang, G.S. Couch, D.M. Greenblatt, E.C. Meng, J. Comput. Chem. **25**, 1605 (2004)
51. G.M. Morris, D.S. Goodsell, R.S. Halliday, J. Comput. Chem. **19**, 1639 (1998)
52. J. Sambrook, E.F. Fritsch, T. Maniatis, *Molecular Cloning: A Laboratory Manual* (Cold Spring Harbor Laboratory, Cold Spring Harbor, NY, 1989)
53. N. Shahabadi, S. Kashanian, F. Darabi, Eur. J. Med. Chem. **45**, 4239 (2010)
54. A. Braca, N. de Tommasi, L. di Bari, C. Pizza, M. Politi, I. Morelli, J. Nat. Prod. **64**, 892 (2001)
55. W.J. Geary, Coordin. Chem. Rev. **7**, 81 (1971)
56. H.P. Ebrahimi, J.S. Hadi, Z.A. Abdulnabi, Z. Bolandnazar, Spectrochim. Acta A **117**, 485 (2014)
57. B.D. Wang, Z.Y. Yang, D.D. Qin, Z.N. Chen, J. Photochem. Photobiol., A **194**, 49 (2008)
58. A.K. Singh, O.P. Pandey, S.K. Sengupta, Spectrochim. Acta A **85**, 1 (2012)
59. D. Arish, M. Sivasankaran Nair, Spectrochim. Acta A **82**, 191 (2011)
60. S. Sobha, R. Mahalakshmi, N. Raman, Spectrochim. Acta A **92**, 175 (2012)
61. D.M.A. El-Aziz, S.E.H. Etaiw, E.A. Ali, J. Mol. Struct. **1048**, 487 (2013)
62. S.E.H. Etaiw, D.M.A. El-Aziz, E.H.A. El-Zaher, E.A. Ali, Spectrochim. Acta A **79**, 1331 (2011)
63. C.J. Dhanaraj, M.S. Nair, J. Saudi Chem. Soc. **18**, 479 (2014)
64. S. Chattopadhyay, G. Bocelli, A. Cantoni, A. Ghosh, Inorg. Chim. Acta **359**, 4441 (2006)
65. R. SelwinJoseyphus, M. Sivasankaran Nair, Arab. J. Chem. **3**, 195 (2010)
66. S.B. Kalia, K. Lumba, G. Kaushal, M. Sharma, Indian J. Chem. A **46A**, 1233 (2007)
67. L.M. Venanzi, J. Inorg. Nucl. Chem. **8**, 137 (1958)
68. O.A.M. Ali, Spectrochim. Acta A **132**, 52 (2014)
69. N. Raman, Y. Pitchaikani Raja, A. Kulandaisamy, Proc. Indian Acad. Sci. (Chem. Sci.) **113**, 183 (2001)
70. K.D. Karlin, J. Zubieta (eds.), *Copper Coordination Chemistry: Biochemical and Inorganic Perspectives* (Adenine Press, Guilderland, NY, 1983)
71. A.M. Mansour, J. Therm. Anal. Calorim. **123**, 571 (2016)
72. A. Majumder, G.M. Rosair, A. Mallick, N. Chattopadhyay, S. Mitra, Polyhedron **25**, 1753 (2006)
73. A.W. Varnes, R.B. Dodson, E.L. Wehry, J. Am. Chem. Soc. **94**, 946 (1972)
74. B.E. Warren, *X–ray Diffraction* (Dover, New York, 1990)
75. B. Mondak, B. Sen, S. Sarkar, E. Zangrando, P. Chattopadhyay, J. Chem. Sci. **129**, 45 (2017)
76. S.E. Sherman, D. Gibson, A.H.J. Wang, S.J. Lippard, J. Am. Chem. Soc. **110**, 7368 (1988)
77. L. Strekowski, B. Wilson, Mutat. Res. **623**, 3 (2007)
78. P.K. Sasmal, A.K. Patra, A.R. Chakravarty, J. Inorg. Biochem. **102**, 1463 (2008)